Integration of a Hydrogenase in a Lead halide Perovskite Photoelectrode for Solar Fuel Synthesis

Esther Edwardes Moore[1], Virgil Andrei[1], Sónia Zacarias[2], Inês A. C. Pereira[2], Erwin Reisner[1*]

[1]Department of Chemistry, University of Cambridge, Lensfield Road, Cambridge CB2 1EW, U.K.

[2]Instituto de Tecnologia Química e Biológica António Xavier, Universidade Nova de Lisboa, Av. da República, 2780-157 Oeiras, Portugal

Corresponding author: reisner@ch.cam.ac.uk

Supporting Information Placeholder

ABSTRACT: Perovskite solar cells are notoriously moisture-sensitive, but recent encapsulation strategies have enabled their application as photoelectrodes in aqueous solution. However, these systems typically rely on precious metal co-catalysts and their combination with biological materials remains elusive. Here, we interface [NiFeSe] hydrogenase from *Desulfovibrio vulgaris* Hildenborough, a highly active enzyme for H_2 generation, with a triple cation mixed halide perovskite. The perovskite-hydrogenase photoelectrode produces a photocurrent of −5 mA cm^{-2} at 0 V *vs.* RHE during AM1.5G irradiation, is stable for 12 h and the hydrogenase exhibits a turnover number of 1.9x10^6. The positive onset potential of +0.8 V *vs.* RHE allows its combination with a $BiVO_4$ water oxidation photoanode to give a self-sustaining, bias-free photoelectrochemical tandem system for overall water splitting. This work demonstrates the compatibility of perovskite elements with biological catalysts to produce hybrid photoelectrodes with benchmark performance, which establishes their utility in semi-artificial photosynthesis.

As a globally abundant, sustainable and economical energy source, solar energy is the fastest growing renewable alternative.[1, 2] Artificial photosynthesis is a process that uses sunlight for the production of renewable chemical fuels, so-called solar fuels, thus addressing the intermittency limitations of photovoltaic (PV) technologies.[3, 4] Solar fuel synthesis can be achieved by direct coupling an efficient light absorber to a fuel-producing catalyst.[5, 6] Organic-inorganic lead halide perovskites have recently received much attention due to their cheap production costs and promising PV cell efficiencies, currently reaching up to 24.2%.[2, 7-10] However, moisture, air and temperature instability has challenged the use of perovskites in photoelectrochemical (PEC) devices.[11-14] Significant improvements have recently been achieved in PEC H_2 production using a perovskite in aqueous solution through the use of protection layers such as Field's metal (FM), Ti foil and epoxy resin.[11-13, 15-22] These encapsulation approaches have extended the operation lifetime of solution immersed perovskite-based photocathodes from seconds to up to 12 h. However, all H_2-evolving PEC perovskite photocathodes have employed high cost, low abundance Pt nanoparticles as the co-catalyst to date.

Semi-artificial photosynthesis combines the evolutionarily-optimized catalytic activity of biological catalysts such as isolated enzymes with synthetic photoabsorbers.[23-26] Hydrogenases (H_2ases) are highly efficient and reversible H_2 production enzymes with a per active-site activity matching Pt.[27-29] The integration of enzymes such as H_2ase with a synthetic photocathode based on Si and Cu_2O has previously been achieved,[30-34] but the combination with a perovskite has remained inaccessible due to the moisture sensitivity of this photoabsorber and difficulty of achieving a productive enzyme-photoabsorber interface.

Here, a perovskite-H_2ase photocathode is presented, realized by an encapsulation system that protects the photoabsorber and provides a biocompatible, bespoke porous scaffold for the enzyme. This semi-artificial photocathode enables combination with a $BiVO_4$ water oxidation photoanode for bias-free, tandem PEC water splitting into H_2 and O_2 (Figure 1).

Optimized cesium formamidinium methylammonium (CsFAMA) triple cation perovskite devices with a FM protection layer were assembled and characterized as previously reported (**Erro! A origem da referência não foi encontrada.**; see Experimental Section and Figure S1 in the Supporting Information for details).[17] Enzymes can be integrated with high loading into hierarchically structured, macro and mesoporous, inverse opal (IO) metal oxide

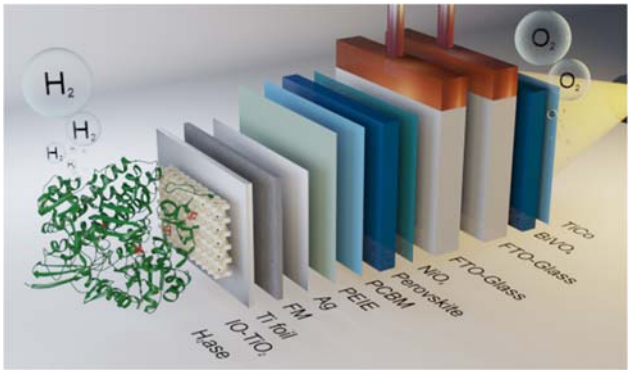

Figure 1. Schematic representation of the tandem PEC cell consisting of a FM-encapsulated perovskite photocathode with H_2ase integrated into an IO-TiO_2 layer and a $BiVO_4$ photoanode. TiCo refers to the water oxidation layer precursor: [$Ti_4O(OEt)_{15}(CoCl)$]. PCBM: [6,6]-phenyl C_{61} butyric acid methyl ester. PEIE: polyethylenimine.

scaffolds.[30, 35, 36] TiO_2 has a sufficiently negative conduction band potential for the reduction of aqueous protons, is stable under reducing conditions and is known to provide an excellent interface with enzymes.[30, 37, 38] The high-temperature (>100 °C) sensitivity of the perovskite prevents *in situ* annealing of the IO-TiO_2 directly on the FM surface. Therefore, anatase TiO_2 nanoparticles (~21 nm Ø) were co-assembled with polystyrene beads (750 nm Ø) on Ti foil and annealed at 500 °C to give Ti|IO-TiO_2 (Figure S2). The geometrical surface area of the IO-TiO_2 scaffold was 0.28 cm^2 with an IO-TiO_2 film thickness of 15 µm. The Ti foil|IO-TiO_2 was then joined to the protected perovskite by briefly melting the FM sheet *via* a Peltier thermoelectric element (at ~70 °C) and an epoxy resin was used to seal the edges to give the encapsulated photocathode: PVK|IO-TiO_2 [FTO-glass|NiO_x|perovskite|PCBM|PEIE|Ag|FM|Ti|IO-TiO_2].

A [NiFeSe] H_2ase from *Desulfovibrio vulgaris* Hildenborough (*Dv*H) was purified and characterized as previously reported,[39] and selected due to its considerable H_2 evolution activity compared to *Dv*H [NiFe] H_2ase.[28, 38, 40-42] This enzyme has improved O_2 tolerance due to the presence of a selenocysteine residue (Sec489) in the active site (Figure S3),[40, 42-45] which is beneficial for its application in overall water splitting. The [NiFeSe] H_2ase (5 µL, 50 pmol) was dropcast onto Ti|IO-TiO_2 and left to saturate the film for 30 min in a N_2 atmosphere. Protein film voltammetry of the Ti|IO-TiO_2|H_2ase electrode in a three-electrode configuration demonstrated that proton reduction occurred with minimal overpotential, indicative of efficient charge transfer at the TiO_2-hydrogenase interface (Figure S4). The Ti|IO-TiO_2|H_2ase electrode displayed excellent current densities (−2.5 mA cm^{-2}) with high stability for several hours at an applied potential (E_{app}) of −0.5 V *vs.* RHE under N_2 (a Faradaic efficiency for H_2, FE_{H_2}, after 24 h of 78% was determined by gas chromatography), including robustness in the presence of O_2. The E_{app} of −0.5 V *vs*. RHE was applied to reflect the estimated perovskite photovoltage of 0.9 V in the PEC experiments, where an E_{app} of +0.4 V *vs*. RHE has been applied (see below).

Protein-film photoelectrochemistry of the PVK|IO-TiO_2|H_2ase photocathode (three-electrode configuration, H_2ase integrated as above) was conducted at 25 °C under chopped simulated solar light irradiation (100 mW cm^{-2}, AM1.5G; back-irradiation). Linear sweep voltammetry (LSV) of the assembled PVK|IO-TiO_2|H_2ase electrode showed a cathodic onset potential at +0.8 V *vs*. RHE and photocurrent densities of −5 mA cm^{-2} at 0 V *vs.* RHE (**Erro! A origem da referência não foi encontrada.**a).

Controlled potential photoelectrolysis (CPPE) was conducted at +0.4 V *vs*. RHE and gas chromatography used to quantify H_2 evolution yields. CPPE demonstrated the stability of the photocathode, which consistently achieved 12 h of stable catalysis (Figure 2b). Failure of the enzyme-photocathode occurred due to water influx into the encapsulated perovskite, characterized by spikes of anodic and cathodic current consistent with previous reports.[15, 17] The H_2ase electrode generated 258 ± 55 μmol_{H_2} cm^{-2} of H_2, whereas the enzyme-free electrode produced <1 μmol_{H_2} cm^{-2}. The FE_{H_2} of PVK|IO-TiO_2|H_2ase after 14 h was (91 ± 1.5)% with a H_2ase-based turnover number (TON_{H_2}) of 1.9×10^6 and turnover frequency (TOF_{H_2}) of 95 s^{-1}. The TON_{H_2} and TOF_{H_2} were calculated based on total H_2ase applied to the IO-TiO_2 scaffold and therefore represent the lower limit of enzyme activity.[31]

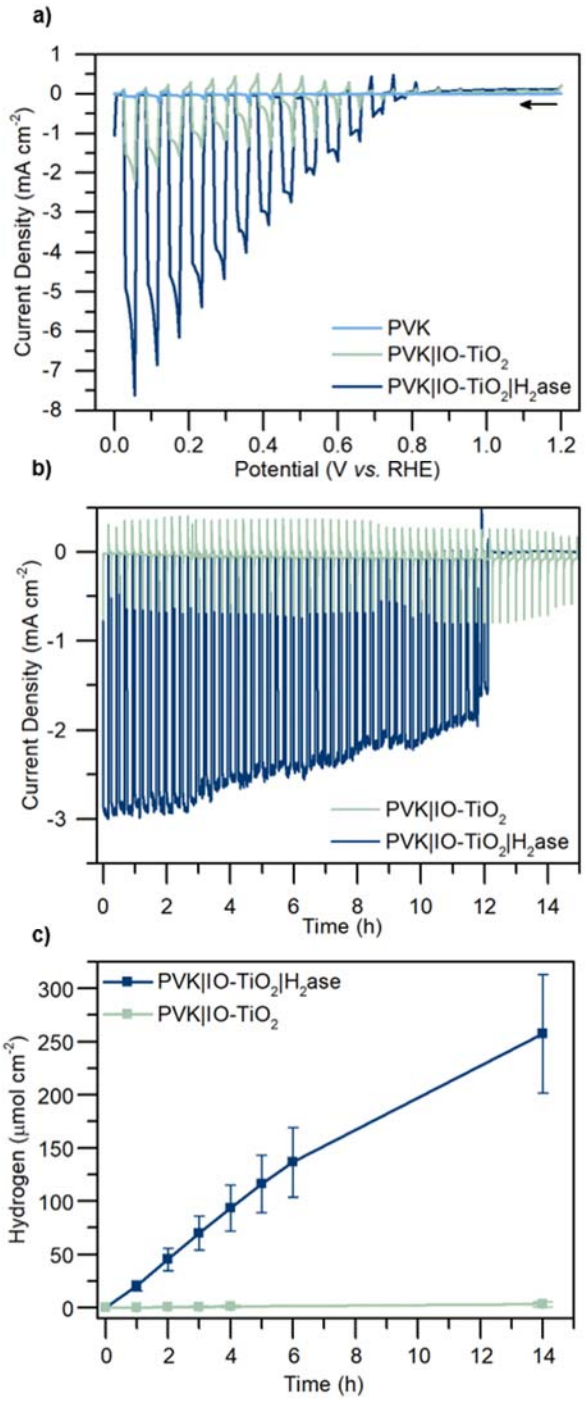

Figure 2. (a) LSV of PVK|IO-TiO_2|H_2ase (blue), PVK|IO-TiO_2 (green), PVK (light blue) electrodes with chopped illumination at a scan rate of 10 mV s^{-1}. (b) CPPE at E_{app} = +0.4 V *vs.* RHE with a dark period lasting 5 min following every 10 min of light exposure. (c) H_2 evolution from CPPE quantified by gas chromatography. Conditions: MES (50 mM, pH 6.0), KCl (50 mM), *Dv*H [NiFeSe] H_2ase (50 pmol), simulated solar light back-irradiation (AM1.5G, 100 mW cm^{-2}), N_2 atmosphere, 25 °C.

Bias-free tandem water splitting has long been a desirable goal for PEC cells.[30, 36, 46, 47] Here a $BiVO_4$-based water oxidation photoanode was prepared by electrodeposition of BiOI, dropcasting and annealing a vanadium precursor and finally

spin-coating a layer of a cobalt-containing co-catalyst as previously reported.[17, 48] PEC analysis of the photoanode (three-electrode set-up; Figure S5) gave an onset potential of +0.1 V *vs*. RHE and a current density of 2.4 mA cm^{-2} at +1.23 V *vs*. RHE.

The positive onset potential of the PVK|IO-TiO_2|H_2ase photocathode is essential for combination with the $BiVO_4$ photoanode to assemble a tandem water splitting PEC device (Figure S6). The robustness of the [NiFeSe] H_2ase toward O_2 provided the possibility to assemble a 'semi-artificial leaf', where the photoelectrodes were not separated into two compartments by a membrane (Figure S4). The $BiVO_4$||PVK|TiO_2|H_2ase tandem cell (**Erro! A origem da referência não foi encontrada.**) was prepared and PEC analysis undertaken in a single compartment cell with illumination through the front of the $BiVO_4$ photoanode. The two-electrode device achieved a current density of 1.1 mA cm^{-2} under bias-free conditions (U_{app} = 0.0 V) and stepped potential chronoamperometry revealed an onset potential of −0.6 V (Figure 3a). Bias-free CPPE showed a gradual decrease in photocurrent over 8 h, which can be attributed to slowly progressing inactivation of the enzyme. In agreement, the current density returned almost to the initial value when a sacrificial electron acceptor (methyl viologen) was added to the tandem PEC cell after prolonged irradiation (Figure S7). The peak FE of the device was (82 ± 3)% for H_2 and (50 ± 8)% for O_2 (FE over time; Figure S8). The $BiVO_4$||PVK|TiO_2|H_2ase cell produced 21.2 ± 3.2 μmol_{H_2} cm^{-2} and 9.0 ± 2.7 μmol_{O_2} cm^{-2} after 8 h CPPE, giving a H_2:O_2 ratio of 2.3.

The PVK|IO-TiO_2|H_2ase photocathode (Figure 4) and $BiVO_4$||PVK|TiO_2|H_2ase tandem device (Figure S9) compares favorably with state-of-the-art H_2 production PEC systems employing earth abundant molecular catalysts (synthetic and biological) in pH benign aqueous solution (see Tables S1 & S2 for details). Three semi-artificial H_2 evolution photocathodes have been previously reported (Figure 4, colored): a [NiFeSe] H_2ase from *Desulfomicrobium baculatum* was introduced onto a p-silicon (p-Si) photoabsorber *via* an IO-TiO_2 scaffold,[30] whereas [FeFe] H_2ases have been combined with both p-type CuO_2 and black-Si photoabsorbers.[31, 32] Of the systems which employed small molecule catalysts (Figure 4, grey-scale), a Ni Dubois-type catalyst applied to a p-Si photoabsorber and a Fe-porphyrin and polymeric Co-based catalysts combined with a GaP photocathode provide state-of-the-art performances.[33, 49, 50] The PVK-H_2ase system here therefore performs superior to equivalent earth-abundant molecular artificial and biological catalyst systems reported to date.

In conclusion, the combination of a biocatalyst with a moisture sensitive perovskite photoabsorber has been accomplished and this bio-material hybrid has subsequently been employed in overall tandem water splitting. The tandem PEC cell was realized by (i) encapsulating the perovskite using a eutectic alloy, metal foil and epoxy resin, (ii) integrating the enzyme into a hierarchical TiO_2 scaffold and (iii) coupling to a suitable photoanode. The PVK|IO-TiO_2|H_2ase system achieved benchmark performance for photocathodes driven by earth abundant catalysts with a current density of −5 mA cm^{-2} at 0.0 V *vs*. RHE, a positive onset of +0.8 V *vs*. RHE, H_2 production yield (258 ± 55 μmol_{H_2} cm^{-2}) and a H_2ase-based TON_{H_2} of 1.9x10^6. A bias-free semi-artificial water splitting H_2 evolution device was produced using the PVK|IO-TiO_2|H_2ase photocathode and a water oxidizing $BiVO_4$ photoanode. In a single compartment 'leaf' configuration, the tandem PEC

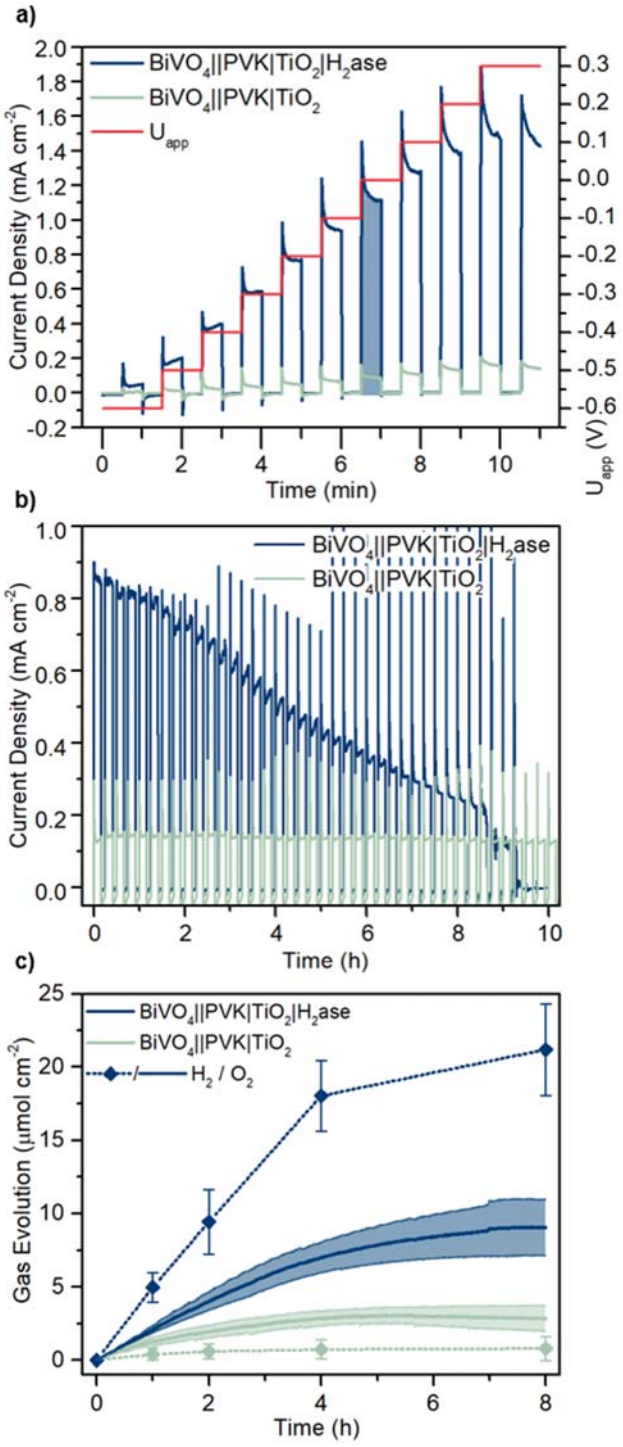

Figure 3. (a) Stepped potential chronoamperometry of $BiVO_4$||PVK|TiO_2|H_2ase (blue) and H_2ase-free $BiVO_4$||PVK|TiO_2 (green) tandem cells from U_{app} = −0.6 V to +0.3 V. The current density at U_{app} = 0.0 V has been highlighted. (b) CPPE of $BiVO_4$||PVK|TiO_2|H_2ase (blue) and H_2ase-free $BiVO_4$||PVK|TiO_2 (green) tandem cells at U_{app} = 0.0 V with a dark period lasting 5 min following every 10 min of light exposure. (c) H_2 (dotted line with measurement points) and O_2 (solid line) evolution from CPPE repeats. Conditions: MES (50 mM, pH 6.0), KCl (50 mM), *Dv*H [NiFeSe] H_2ase (50 pmol), simulated solar light irradiation (AM1.5G, 100 mW cm^{-2}), N_2 atmosphere, 25 °C.

system was shown to be potential generating with an onset potential of −0.6 V and produced current densities of 1.1 mA cm^{-2} without electrochemical bias. This work provides a new benchmark for photocathodes and tandem PEC devices employing earth-abundant molecular H_2 production catalysts,

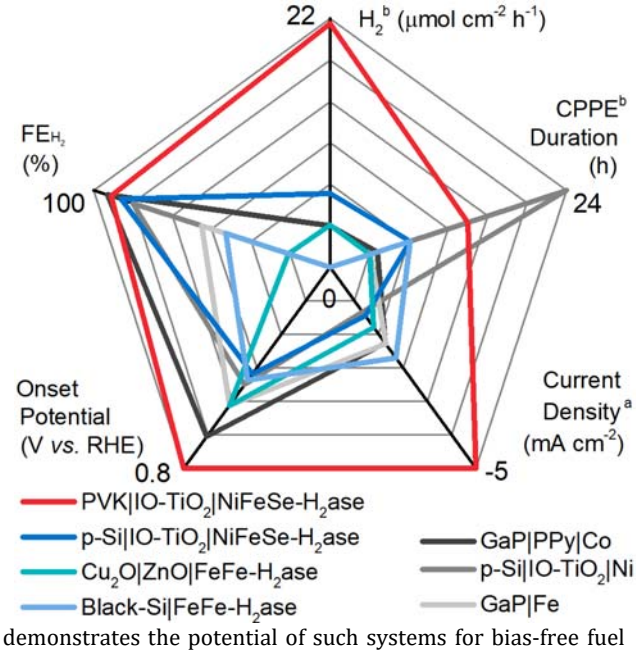

demonstrates the potential of such systems for bias-free fuel production and establishes perovskites as a suitable photoelectrode materials for the integration of biocatalysts.

Figure 4. Comparison of the PVK|IO-TiO_2|H_2ase photocathode with state-of-the-art electrodes that employ immobilized earth abundant molecular H_2 evolution catalysts. Each axis has been scaled between zero and the maximum value displayed (benchmark value). Lines passing through the center indicate value was not available. To validate comparison H_2 evolution was calculated per hour. See Table S1 for details. a) Current density measured at E_{app}, given in Table S1, extracted from LSV measurements. b) Extracted from CPPE measurements. Comparison of the $BiVO_4$||PVK|TiO_2|H_2ase tandem cell with previously reported systems can be found as Figure S9 in the Supporting Information.

ASSOCIATED CONTENT

Supporting Information

The Supporting Information is available free of charge on the ACS Publications website at DOI:

.

Supporting Figures & Tables (PDF)

AUTHOR INFORMATION

Corresponding Author

*reisner@ch.cam.ac.uk

Notes

The authors declare no competing financial interests.

ACKNOWLEDGMENT

This work was supported by an ERC Consolidator Grant "MatEnSAP" (E.E.M., E.R.), the University of Cambridge (Vice-Chancellor and Winton scholarships to V.A.), XX Portugal XX.

REFERENCES

1. Coyle, E. D.; Simmons, R. A., *Understanding the Global Energy Crisis*. Purdue University Press: Lafayette, March 2014.
2. Nayak, P. K.; Mahesh, S.; Snaith, H. J.; Cahen, D., Photovoltaic solar cell technologies: analysing the state of the art. *Nat. Rev. Mater.* **2019,** *4*, 269.
3. Tachibana, Y.; Vayssieres, L.; Durrant, J. R., Artificial photosynthesis for solar water-splitting. *Nat. Photon.* **2012,** *6*, 511-518.
4. Dalle, K. E.; Warnan, J.; Leung, J. J.; Reuillard, B.; Karmel, I. S.; Reisner, E., Electro- and Solar-driven Fuel Synthesis with First Row Transition Metal Complexes. *Chem. Rev.* **2019,** *119* (4), 2752-2875.
5. Jia, J.; Seitz, L. C.; Benck, J. D.; Huo, Y.; Chen, Y.; Ng, J. W. D.; Bilir, T.; Harris, J. S.; Jaramillo, T. F., Solar water splitting by photovoltaic-electrolysis with a solar-to-hydrogen efficiency over 30%. *Nat. Commun.* **2016,** *7*, 13237.
6. Hisatomi, T.; Kubota, J.; Domen, K., Recent advances in semiconductors for photocatalytic and photoelectrochemical water splitting. *Chem. Soc. Rev.* **2014,** *43* (22), 7520-7535.
7. National Renewable Energy Laboratory. https://www.nrel.gov/pv/assets/pdfs/best-research-cell-efficiencies-190416.pdf (accessed June 2019).
8. Green, M. A.; Ho-Baillie, A.; Snaith, H. J., The emergence of perovskite solar cells. *Nat. Photonics* **2014,** *8*, 506-514.
9. Jiang, Q.; Chu, Z.; Wang, P.; Yang, X.; Liu, H.; Wang, Y.; Yin, Z.; Wu, J.; Zhang, X.; You, J., Planar-Structure Perovskite Solar Cells with Efficiency beyond 21%. *Adv. Mater.* **2017,** *29*, 1703852.
10. Kim, H.-S.; Hagfeldt, A.; Park, N.-G., Morphological and compositional progress in halide perovskite solar cells. *Chem. Commun.* **2019,** *55*, 1192-1200.
11. Da, P.; Cha, M.; Sun, L.; Wu, Y.; Wang, Z. S.; Zheng, G., High-performance perovskite photoanode enabled by Ni passivation and catalysis. *Nano. Lett.* **2015,** *15* (5), 3452-3457.
12. Hoang, M. T.; Pham, N. D.; Han, J. H.; Gardner, J. M.; Oh, I., Integrated Photoelectrolysis of Water Implemented On Organic Metal Halide Perovskite Photoelectrode. *ACS Appl. Mater. Interfaces* **2016,** *8* (19), 11904-11909.
13. Wang, C.; Yang, S.; Chen, X.; Wen, T.; Yang, H. G., Surface-functionalized perovskite films for stable photoelectrochemical water splitting. *J. Mater. Chem. A* **2017,** *5* (3), 910-913.
14. Correa-Baena, J.-P.; Abate, A.; Saliba, M.; Tress, W.; Jacobsson, T. J.; Grätzel, M.; Hagfeldt, A., The rapid evolution of highly efficient perovskite solar cells. *Energy Environ. Sci.* **2017,** *10*, 710-727.
15. Crespo-Quesada, M.; Pazos-Outón, L. M.; Warnan, J.; Kuehnel, M. F.; Friend, R. H.; Reisner, E., Metal-encapsulated organolead halide perovskite photocathode for solar-driven hydrogen evolution in water. *Nat. Commun.* **2016,** *7*, 12555.
16. Zhang, H.; Yang, Z.; Yu, W.; Wang, H.; Ma, W.; Zong, X.; Li, C., A Sandwich-Like Organolead Halide Perovskite Photocathode for Efficient and Durable Photoelectrochemical Hydrogen Evolution in Water. *Adv. Energy Mater.* **2018,** *8*, 1800795.

17. Andrei, V.; Hoye, R. L. Z.; Crespo-Quesada, M.; Bajada, M.; Ahmad, S.; Volder, M. D.; Friend, R.; Reisner, E., Scalable Triple Cation Mixed Halide Perovskite–BiVO4 Tandems for Bias-Free Water Splitting. *Adv. Energy Mater.* **2018,** *8*, 1801403.
18. Poli, I.; Hintermair, U.; Regue, M.; Kumar, S.; Sackville, E. V.; Baker, J.; Watson, T. M.; Eslava, S.; Cameron, P. J., Graphite-protected $CsPbBr_3$ perovskite photoanodes functionalised with water oxidation catalyst for oxygen evolution in water. *Nat. Commun.* **2019,** *10*, 2097.
19. Koh, T. M.; Shanmugam, V.; Guo, X.; Lim, S. S.; Filonik, O.; Herzig, E. M.; Müller-Buschbaum, P.; Swamy, V.; Chien, S. T.; Mhaisalkar, S. G.; Mathews, N., Enhancing moisture tolerance in efficient hybrid 3D/2D perovskite photovoltaics. *J. Mater. Chem. A* **2018,** *6*, 2122-2128.
20. Chen, J.; Yin, J.; Zheng, X.; Ahsaine, H. A.; Zhou, Y.; Dong, C.; Mohammed, O. F.; Takanabe, K.; Bakr, O. M., Compositionally Screened Eutectic Catalytic Coatings on Halide Perovskite Photocathodes for Photoassisted Selective CO_2 Reduction. *ACS Energy lett.* **2019,** *4* (6), 1279-1286.
21. Crespo-Quesada, M.; Reisner, E., Emerging approaches to stabilise photocorrodible electrodes and catalysts for solar fuel applications. *Energy Environ. Sci.* **2017,** *10*, 1116-1127.
22. Ahmad, S.; Sadhanala, A.; Hoye, R. L. Z.; Andrei, V.; Modarres, M. H.; Zhao, B.; Rongé, J.; Friend, R. H.; Volder, M. D., Triple Cation based Perovskite Photocathodes with AZO Protective Layer for Hydrogen Production Applications. *ACS Appl. Mater. Interfaces* **2019**, Accepted Manuscript. DOI: 10.1021/acsami.9b04963.
23. Kornienko, N.; Zhang, J. Z.; Sakimoto, K. K.; Yang, P.; Reisner, E., Interfacing nature's catalytic machinery with synthetic materials for semi-artificial photosynthesis. *Nat. Nanotech.* **2018,** *13*, 890-899.
24. Evans, R. M.; Siritanaratkul, B.; Megarity, C. F.; Pandey, K.; Esterle, T. F.; Badiani, S.; Armstrong, F. A., The value of enzymes in solar fuels research – efficient electrocatalysts through evolution. *Chem. Soc. Rev.* **2019,** *48*, 2039-2052.
25. Kim, J. H.; Na, D. H.; Park, C. B., Nanobiocatalytic assemblies for artificial photosynthesis. *Curr. Opin. Biotechnol.* **2014,** *28*, 1-9.
26. Lee, S. H.; Choi, D. S.; Kuk, S. K.; Park, C. B., Photobiocatalysis: Activating Redox Enzymes by Direct or Indirect Transfer of Photoinduced Electrons. *Angew. Chem. Int. Ed.* **2018,** *57* (27), 7958-7985.
27. Tran, P. D.; Barber, J., Proton reduction to hydrogen in biological and chemical systems. *Phys. Chem. Chem. Phys.* **2012,** *14*, 13772-13784.
28. Lubitz, W.; Ogata, H.; Rüdiger, O.; Reijerse, E., Hydrogenases. *Chem. Rev.* **2014,** *114*, 4081-4148.
29. Jones, A. K.; Sillery, E.; Albracht, S. P. J.; Armstrong, F. A., Direct comparison of the electrocatalytic oxidation of hydrogen by an enzyme and a platinum catalyst. *Chem. Commun.* **2002**, 866-867.
30. Nam, D. H.; Zhang, J. Z.; Andrei, V.; Kornienko, N.; Heidary, N.; Wagner, A.; Nakanishi, K.; Sokol, K. P.; Slater, B.; Zebger, I.; Hofmann, S.; Fontecilla-Camps, J. C.; Park, C. B.; Reisner, E., Solar Water Splitting with a Hydrogenase Integrated in Photoelectrochemical Tandem Cells. *Angew. Chem. Int. Ed.* **2018,** *57*, 10595-10599.
31. Zhao, Y.; Anderson, N. C.; Ratzloff, M. W.; Mulder, D. W.; Zhu, K.; Turner, J. A.; Neale, N. R.; King, P. W.; Branz, H. M., Proton Reduction Using a Hydrogenase-Modified Nanoporous Black Silicon Photoelectrode. *ACS Appl. Mater. Interfaces* **2016,** *8* (23), 14481−14487.
32. Tiana, L.; Németh, B.; Berggren, G.; Tian, H., Hydrogen evolution by a photoelectrochemical cell based on a Cu2O-ZnO-[FeFe] hydrogenase electrode. *J. Photochem. Photobiol. A: Chem.* **2018,** *366*, 27-33.
33. Leung, J. J.; Warnan, J.; Nam, D. H.; Zhang, J. Z.; Willkomm, J.; Reisner, E., Photoelectrocatalytic H_2 evolution in water with molecular catalysts immobilised on p-Si *via* a stabilising mesoporous TiO_2 interlayer. *Chem. Sci.* **2017,** *8*, 5172-5180.
34. Lee, C. Y.; Park, H. S.; Fontecilla-Camps, J. C.; Reisner, E., Photoelectrochemical H_2 Evolution with a Hydrogenase Immobilized on a TiO_2-Protected Silicon Electrode. *Angew. Chem. Int. Ed.* **2016,** *55* (20), 5971-5974.
35. Mersch, D.; Lee, C.-Y.; Zhang, J. Z.; Brinkert, K.; Fontecilla-Camps, J. C.; Rutherford, A. W.; Reisner, E., Wiring of Photosystem II to Hydrogenase for Photoelectrochemical Water Splitting. *J. Am. Chem. Soc.* **2015,** *137*, 8541–8549.
36. Sokol, K. P.; Robinson, W. E.; Warnan, J.; Kornienko, N.; Nowaczyk, M. M.; Ruff, A.; Zhang, J. Z.; Reisner, E., Bias-free photoelectrochemical water splitting with photosystem II on a dye-sensitized photoanode wired to hydrogenase. *Nat. Energy* **2018,** *3*, 944-951.
37. Miller, M.; Robinson, W. E.; Oliveira, A. R.; Heidary, N.; Kornienko, N.; Warnan, J.; Pereira, I. A. C.; Reisner, E., Interfacing Formate Dehydrogenase with Metal Oxides for the Reversible Electrocatalysis and Solar-Driven Reduction of Carbon Dioxide. *Angew. Chem. Int. Ed.* **2019,** *131* (14), 4649-4653.
38. Wombwell, C.; Caputo, C. A.; Reisner, E., [NiFeSe]-Hydrogenase Chemistry. *Acc. Chem. Res.* **2015,** *48*, 2858–2865.
39. Zacarias, S.; Véle, M.; Pita, M.; Lacey, A. L. D.; Matias, P. M.; Pereira, I. A. C., Characterization of the [NiFeSe] hydrogenase from *Desulfovibrio vulgaris* Hildenborough. *Meth. Enzymol.* **2018,** *613*, 169-201.
40. Gutierrez-Sanchez, C.; Rudiger, O.; Fernandez, V. M.; De Lacey, A. L.; Marques, M.; Pereira, I. A., Interaction of the active site of the Ni-Fe-Se hydrogenase from *Desulfovibrio vulgaris* Hildenborough with carbon monoxide and oxygen inhibitors. *J. Biol. Inorg. Chem.* **2010,** *15* (8), 1285-1292.
41. Valente, F. M. A.; Oliveira, A. S. F.; Gnadt, N.; Pacheco, I.; Coelho, A. V.; Xavier, A. V.; Teixeira, M.; Soares, C. M.; Pereira, I. A. C., Hydrogenases in *Desulfovibrio vulgaris* Hildenborough: structural and physiologic characterisation of the membrane-bound [NiFeSe] hydrogenase. *J. Biol. Inorg. Chem.* **2005,** *10* (6), 667-682.
42. Marques, M. C.; Tapia, C.; Gutiérrez-Sanz, O.; Ramos, A. R.; Keller, K. L.; Wall, J. D.; Lacey, A. L. D.; Matias, P. M.; Pereira, I. A. C., The direct role of selenocysteine in [NiFeSe] hydrogenase maturation and catalysis. *Nat. Chem. Biol.* **2017,** *13*, 544-550.
43. Marques, M. C.; Coelho, R.; De Lacey, A. L.; Pereira, I. A.; Matias, P. M., The three-dimensional structure of [NiFeSe] hydrogenase from *Desulfovibrio vulgaris* Hildenborough: a hydrogenase without a bridging ligand in the active site in its oxidised, "as-isolated" state. *J. Mol. Biol.* **2010,** *396* (4), 893-907.
44. De Lacey, A. L.; Gutierrez-Sanchez, C.; Fernandez, V. M.; Pacheco, I.; Pereira, I. A., FTIR spectroelectrochemical characterization of the Ni-Fe-Se hydrogenase from *Desulfovibrio vulgaris* Hildenborough. *J. Biol. Inorg. Chem.* **2008,** *13* (8), 1315-1320.
45. Parkin, A.; Goldet, G.; Cavazza, C.; Fontecilla-Camps, J. C.; Armstrong, F. A., The Difference a Se Makes? Oxygen-Tolerant Hydrogen Production by the [NiFeSe]-Hydrogenase

from *Desulfomicrobium baculatum*. *J. Am. Chem. Soc.* **2008,** *130* (40), 13410-13416.
46. Li, F.; Fan, K.; Xu, B.; Gabrielsson, E.; Daniel, Q.; Li, L.; Sun, L., Organic Dye-Sensitized Tandem Photoelectrochemical Cell for Light Driven Total Water Splitting. *J. Am. Chem. Soc.* **2015,** *137*, 9153-9159.
47. Zhang, K.; Ma, M.; Li, P.; Wang, D. H.; Park, J. H., Water Splitting Progress in Tandem Devices: Moving Photolysis beyond Electrolysis. *Adv. Energy Mater.* **2016,** *6* (15), 1600602.
48. Lai, Y. H.; Palm, D. W.; Reisner, E., Multifunctional Coatings from Scalable Single Source Precursor Chemistry in Tandem Photoelectrochemical Water Splitting. *Adv. Energy Mater.* **2015,** *5* (24), 1501668.
49. Khusnutdinova, D.; Beiler, A. M.; Wadsworth, B. L.; Jacob, S. I.; Moore, G. F., Metalloporphyrin-modified semiconductors for solar fuel production. *Chem. Sci.* **2017,** *8*, 253-259.
50. Beiler, A. M.; Khusnutdinova, D.; Wadsworth, B. L.; Moore, G. F., Cobalt Porphyrin–Polypyridyl Surface Coatings for Photoelectrosynthetic Hydrogen Production. *Inorg. Chem.* **2017,** *56* (20), 12178-12185.

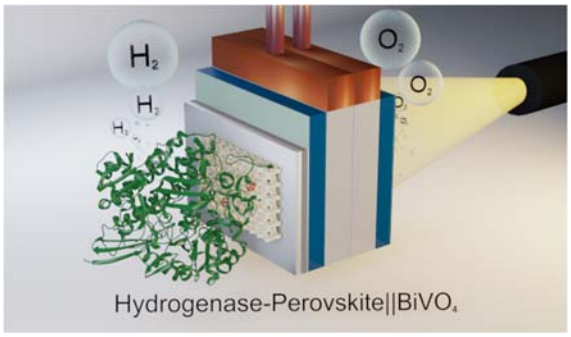
H2
O2
O2
Hydrogenase-Perovskite||BiVO4